**Biogeosciences
Discussions**

Accounting for spatial variation in vegetation properties improves simulations of Amazon forest biomass and productivity in a global vegetation model

A. D. de Almeida Castanho[1], M. T. Coe[1], M. Heil Costa[2], Y. Malhi[3], D. Galbraith[4], and C. A. Quesada[5,4]

[1]The Woods Hole Research Center, 149 Woods Hole Rd., Falmouth, MA 02540, USA
[2]Departamento de Engenharia Agrícola, Universidade Federal de Viçosa (UFV), Viçosa, MG, Brazil
[3]Environmental Change Institute, School of Geography and the Environment, University of Oxford, Oxford, UK
[4]School of Geography, University of Leeds, Leeds, UK
[5]Instituto Nacional de Pesquisas da Amazônia, Manaus, Brazil

Amazon Heterogeneity

A. D. de Almeida Castanho et al.

Title Page

Abstract | Introduction

Conclusions | References

Tables | Figures

◀ | ▶

◀ | ▶

Back | Close

Full Screen / Esc

Printer-friendly Version

Interactive Discussion

**Amazon
Heterogeneity**

A. D. de Almeida
Castanho et al.

Full Screen / Esc

Abstract

Dynamic vegetation models forced with spatially homogeneous biophysical parameters are capable of producing average productivity and biomass values for the Amazon basin forest biome that are close to the observed estimates, but are unable to reproduce the observed spatial variability. Recent observational studies have shown substantial regional spatial variability of above-ground productivity and biomass across the Amazon basin, which is believed to be primarily driven by soil physical and chemical properties. In this study, spatial heterogeneity of vegetation properties is added to the IBIS land surface model, and the simulated productivity and biomass of the Amazon basin are compared to observations from undisturbed forest. The maximum Rubisco carboxylation capacity (V_{cmax}) and the woody biomass residence time (τ_w) were found to be the most important properties determining the modeled spatial variation of above-ground woody net primary productivity and biomass, respectively. Spatial heterogeneity of these properties may lead to a spatial variability of 1.8 times in the simulated woody net primary productivity and 2.8 times in the woody above-ground biomass. The coefficient of correlation between the modeled and observed woody productivity improved from 0.10 with homogeneous parameters to 0.73 with spatially heterogeneous parameters, while the coefficient of correlation between the simulated and observed woody above-ground biomass improved from 0.33 to 0.88. The results from our analyses with the IBIS dynamic vegetation model demonstrate that using single values for key ecological parameters in the tropical forest biome severely limits simulation accuracy. We emphasize that our approach must be viewed as an important first step and that a clearer understanding of the biophysical mechanisms that drive the spatial variability of carbon allocation, τ_w and V_{cmax} are necessary.

1 Introduction

Tropical forests play an important role in the global carbon cycle, accounting for about one third of the global net primary productivity and 55 % of total global forest carbon (Pan et al., 2011; Malhi, 2010). The Amazonia hosts about 50 % of the world's tropi-
5 cal forests (Pan et al., 2011). It is highly diverse in terms of climate, soil physical and chemical properties, and species composition (Davidson et al., 2012; Quesada et al., 2011; Fyllas et al., 2009; Phillips et al., 2004). However, most global vegetation models represent Amazon rainforests through a single set of parameters which do not vary in space and thus fail to represent its complex spatial diversity. Dynamic Global Vege-
10 tation Models (DGVMs) are powerful tools for understanding past and potential future carbon fluxes and stocks. An accurate representation of the spatial heterogeneity and the temporal variability of the forest biophysical properties are essential for useful prediction of the future carbon cycle of Amazon forests. In this work we investigate the importance of representing spatial heterogeneity in vegetation properties in a commonly
15 used DGVM.

Field observations from undisturbed old-growth Amazonian forest plots have recently reported on the regional variation of many forest geomorphological attributes such as: geological history (Higgins et al., 2011), soil properties (Quesada et al., 2011), foliar physiological properties (Fyllas et al., 2009; Lloyd et al., 2010), above-ground
20 live biomass (Malhi et al., 2006; Baker et al., 2004b), above-ground wood productivity (Malhi et al., 2004), net primary productivity (Aragão et al., 2009; Malhi et al., 2009), and vegetation turnover rates (Phillips et al., 2004; Galbraith et al., 2012). These analyses have shown a general east-to-west gradient of tree structure and dynamics in Amazonian forests. Forests in the west tend to have higher above-ground productiv-
25 ity and lower above-ground biomass, while those in the East and Central Amazon are slower growing with higher above-ground biomass (Quesada et al., 2012; Malhi et al., 2004; Baker et al., 2004a). Although the spatial variation in biomass and productivity has been measured and described, the underlying mechanisms are still not well

understood (Malhi, 2012). The east-west gradient appears driven by soil fertility and soil physical properties rather than by climate (Quesada et al., 2011), the soil properties in turn appear to be related to geological history and the exposure of more fertile Miocene-age marine or lacustrine sediments in Western Amazonia (Higgins et al., 2011).

There are some mechanisms that have been discussed in literature to address the spatial variability of woody net primary productivity. The large spatial variability in wood productivity could be directly related to a shift in the balance of carbon allocation between roots and wood and or the respiration rate (Malhi et al., 2004). NPP_w spatial variability could be driven by a variability in gross primary productivity (GPP) due to a potential limitation of photosynthesis by soil P availability (Quesada et al., 2012; Mercado et al., 2011; Lloyd et al., 2001, 2010). Malhi et al. (2004) data analyses also suggest that carbon use efficiency (CUE = NPP/GPP) is higher in the west, which means that besides a potentially higher GPP in the western region there is also a potentially higher autotrophic respiration rates in the lower fertile soils of Central Amazonia, making the CUE less efficient there. The direct effect of climate factors such as temperature, short wave radiation and precipitation have been argued to be too small to explain the observed variability in the productivity (Malhi et al., 2004; Senna et al., 2009; Quesada et al., 2012; Galbraith et al., 2012).

The spatial variability of above-ground biomass across the Amazon basin has also been addressed in the literature. Field data have indicated the importance of wood density, canopy height and plant allometry in the biomass estimates (Baker et al., 2004b; Malhi et al., 2006; Feldpausch et al., 2011). Plant turnover rates have been suggested to be important factor for better representation of above-ground biomass in vegetation models (Delbart et al., 2010). This is because field data show that the fast-growing forests in the Western Amazon have lower wood density, lower residence time and therefore lower above-ground biomass than the slow growing forest in Central and Eastern Amazonia (Phillips et al., 2004). The mechanisms that determine the spatial variability in plant residence time are still unresolved (Galbraith et al., 2012), it may

Amazon Heterogeneity

A. D. de Almeida Castanho et al.

Title Page

Abstract | Introduction

Conclusions | References

Tables | Figures

|◄ | ►|

◄ | ►

Back | Close

Full Screen / Esc

Printer-friendly Version

Interactive Discussion

be extrinsic factors such as soil physical properties, or disturbance, such as landslides and erosion on steep slopes, or climate directly affecting tree mortality rates, or intrinsic factors such as high growth rates intensifying light competition and associated tree mortality. Residence time is strongly correlated with soil physical properties, and forest growth rates are strongly related to available soil P and climate. However the large-scale variation in biomass appears not to be explained by any of the edaphic properties alone (Quesada et al., 2012).

Dynamic global vegetation models tend to characterize the Amazon forest as a single plant functional type (PFT). A PFT is characterized by a set of parameters that is invariant in space and time. There is a growing awareness that such an approach is unable to capture spatial variations (Senna et al., 2009; Delbart et al., 2010; Fyllas et al., 2012). In this paper we present a novel spatial varying parameterization to simulate the biomass dynamics of Amazonia. In a first step we use the Integrated Biosphere Simulator (IBIS) DGVM with a number of Amazonian sites observational estimates of key biophysical parameters (woody biomass residence time (τ_w), maximum Rubisco carboxylation capacity (V_{cmax}), NPP allocation to wood). In a second step we evaluate which parameters are most important for simulating the spatial variability of above-ground woody net primary productivity and biomass. Finally we create basin-wide raster data sets of the key parameters from the site-specific heterogeneous parameterizations and evaluate their impact on basin-wide simulations of above-ground woody productivity and biomass.

2 Material and methods

The study area is the Amazon region (Fig. 1). The spatial analyses applied here are at $1° \times 1°$ grid cell horizontal resolution. In this section we describe: (1) the IBIS dynamic vegetation model used; (2) the field data used in calibration and validation; and (3) the sequence of model setup and simulations exercises.

2.1 IBIS 2.6. – Integrated Biosphere Simulator

The Integrated Biosphere Simulator (IBIS) is a comprehensive model of terrestrial biospheric processes (Foley et al., 1996; Kucharik et al., 2000). The model uses an integrated framework based on land surface biophysics (canopy and soil physics, plant physiology), vegetation phenology, vegetation dynamics and competition, terrestrial carbon and nutrient cycling. IBIS has been validated and applied to the Amazon (Senna et al., 2009; Delire and Foley, 1999; Foley et al., 2002; Coe et al., 2008). Detailed descriptions of the model can be found in the above publications.

The land surface module was derived from the land surface transfer model (LSX) (Thompson and Pollard, 1995a,b). Land surface processes are represented by two vegetation layers (woody and herbaceous plants), and six soil layers (to simulate the diurnal and seasonal variations of heat and moisture in the total soil depth). The dynamics of soil volumetric water content are simulated for each layer. The soil water infiltration rate is based on the Green–Ampt formulation (Green and Ampt, 1911; Li et al., 2005, 2006). The model has 12 plant functional types (PFT) that compete for light and water using different ecological strategies, while nutrient competition is not currently included. The model allows the coexistence of one or more PFTs per grid cell that combined define a vegetation type. The PFT varies from tropical trees, temperate trees, boreal trees, shrubs through grasses. IBIS represents the Amazonian Forest as a single vegetation type (tropical broadleaf evergreen forest) with spatially homogeneous parameters for key processes. The goal of this study is to clarify the importance of using more detailed spatially-varying parameters within the single plant functional type.

2.2 Field observation database and basin-wide extrapolations

We have assembled a wide range of published data from field observations on several sites across the Amazon basin (Fig. 1). The sites are all in undisturbed old-growth forest, with most of them being part of the RAINFOR network ("Rede Amazónica de

Amazon Heterogeneity

A. D. de Almeida Castanho et al.

Title Page

Abstract | Introduction

Conclusions | References

Tables | Figures

◄ | ►

◄ | ►

Back | Close

Full Screen / Esc

Printer-friendly Version

Interactive Discussion

Inventarios Forestales", Amazon Forest Inventory Network; http://www.rainfor.org). The RAINFOR project is an international effort to monitor structure, composition and dynamics of the Amazonian forest in order to better understand their relationship to soil and climate (Malhi et al., 2002; Peacock et al., 2007). The RAINFOR field data are in general based on one hectare plots (see references for more detailed information). In this study these plot data are aggregated to the one by one degree resolution used in this work in IBIS.

There are few plot measurements of carbon allocation to stems, roots, and leaves reported in the literature. Malhi et al. (2011) compiled a carbon allocation database for tropical forests worldwide. They report the partition of carbon between wood, fine roots and leaves for 10 plots in the Amazonian basin that represent 6 sites at the $1° \times 1°$ grid cell resolution of the model (Table 1). The authors showed that in general there is close-to-equal allocation of new carbon between wood, leaves and fine roots. Aragão et al. (2009) suggested that the C allocation partition appears not related to soil fertility but to soil texture. The authors identified that the allocation of carbon to roots is significantly correlated and decreases with increasing soil clay content. They argue that this happens because, in a sandy soil, roots grow with less resistance from the soil and have faster water absorption in fast-draining sandy soils. For similar reasons and following similar analyses, we observed a high correlation between carbon in fine roots with soil sand percentage and also carbon in leaves with soil sand percentage, shown in Fig. (2) and respective equations (Eq. 1 in Table 1). The carbon allocation between wood, leaves and fine roots for the whole basin are estimated based on the regressions (Eq. 1, Table 1) applied over the soil texture map (Quesada et al., 2010). The correlations between carbon allocation and soil texture are limited to a small number of sites, and may be limited by other factors that are still not well known, or not well represented by this limited database. Considering this hypothesis, that carbon allocation would be related to soil texture, the estimated woody carbon allocation map varies predominantly from 30–40 % carbon allocated to wood and does not reproduce the amplitude of the site specific measurement of carbon allocation (25–50 %) (Fig. 5a). This means that

the effect of assuming this hypothesis is not going to critically affect the final results (Supplement, Table B).

Tree turnover rate has been estimated from field measurements and a strong spatial variability has been reported (25–100 yr) (Phillips et al., 2004). Spatially varying woody biomass residence time (τ_w) is included as an input parameterization in the model. In this work we use the compiled data on τ_w from Galbraith et al. (2012), which is in terms of carbon residence time more appropriate for this study. The dataset comprise analyses of 129 plots across Amazonia for 5–25 yr time series between 1971–2011 (Table 1) (Galbraith et al., 2012). There are 34 $1° \times 1°$ grid cells associated with these sites (Fig. 1). There are strong indications that the τ_w is correlated to soil physical properties (Quesada et al., 2012); however the mechanisms that would explain the spatial variability of τ_w are not completely understood (Quesada et al., 2012, Galbraith et al., 2012). For this reason we opted to scale up the τ_w to the entire basin using simple kriging interpolation of the field data points (Fig. 5b).

Phosphorus (P) is known to be a limiting factor for productivity of mature tropical forests (Vitousek, 1984; Lloyd et al., 2010; Mercado et al., 2011) therefore it is used in this study to represent soil fertility limitation in our model. The total available P in this work is used to estimate the maximum carboxylation capacity of Rubisco. Quesada et al. (2010) performed extensive collection and analyses of soil data at 71 sites with varying soil properties throughout Amazonia. The 71 sites are grouped into 26 $1° \times 1°$ grid cells (Table 1, Fig. 1). Based on field database (Quesada et al., 2010, 2011) we defined a relationship between total soil P measured (average to depth from 0 to 0.3 m) at the site level and the respective soil class (Fig. 3).

Quesada et al. (2011) presented a map of basin wide-distribution of soil coverage for each Reference Soil Group. Based on the relation derived in Fig. 3 and the soil class map, we created a spatial map of total soil P content (average to depth from 0 to 0.3 m) of each $1° \times 1°$ grid cell in the Amazon (Fig. 4). Due to the large variability of soil types within the grid cell we expect to see discrepancies between the site level measurement and the upscaled P obtained for the grid cell based on the soil class. The derived

Amazon Heterogeneity

A. D. de Almeida Castanho et al.

total soil P map qualitatively reproduces the east ($100\,\text{mg}\,\text{kg}^{-1}$) to west ($450\,\text{mg}\,\text{kg}^{-1}$) increase in fertility as observed in the independent site level measurements. Lowest total P soil values occur in Northern Brazil and Southern Venezuela that coincides where the soil sand content is highest (Fig. 4). Total derived P values are estimated to
5 exceed $300\,\text{mg}\,\text{kg}^{-1}$ in a portion of Central Amazonia but there are no observations to corroborate these values. Lacking further field measurements to validate our map, we use it cautiously in this study as a means of understanding the sensitivity of simulated biomass to fertility variation.

Maximum carboxylation capacity of Rubisco (V_{cmax}) and Specific Leaf Area Index
10 (SLA) are important properties for simulating photosynthesis. We collected the existing data on these to explore their spatial distribution in the Amazon Basin to be used as input parameterization in the model. Fyllas et al. (2009) analyzed leaf properties at 62 RAINFOR plots across the Amazon Basin. These data, when averaged to our grid cell of $1° × 1°$, represent 22 data points (Fig. 1, Table 1). The authors present data for leaf
15 mass per unit area (the inverse of the specific leaf area, SLA), and leaf concentration of the main growth limiting nutrients such as N and P. Their analyses showed that, among various environmental components, soil fertility is one of the most important predictors for observed higher nutrient concentration in leaves. Mercado et al. (2009) noted a correlation between V_{cmax} observed from the field and the concentrations of P
20 in leaves. Following the Mercado et al. (2009, 2011) procedure we performed a similar regression equation but between V_{cmax} and total P concentration in soil instead of the P concentration in leaves (Fig. 3b, Eq. 2 in Table 1).

The advantage of this empirical regression with respect to soil P is the ability to estimate V_{cmax} for the whole basin based on Eq. (2) (Table 1) and the map of total soil P
25 concentration (Fig. 4). The V_{cmax} spatial distribution shows the same spatial structure as the P map since the V_{cmax} has been estimated as a linear function of P, with a gradient from west to east (Fig. 5c). There is in general a good agreement between field estimates of V_{cmax} (Mercado et al., 2009) and the estimated map in this work (Fig. 5c). The San Carlos do Rio Negro (SCR, Venezuela) site represents a significant outlier,

Full Screen / Esc

Printer-friendly Version

Interactive Discussion

**Amazon
Heterogeneity**

A. D. de Almeida
Castanho et al.

as the observed V_{cmax} at this site (ranging around $65\,\mu mol\,m^{-2}\,s^{-1}$, Mercado et al., 2011) is considerably higher than that estimated value based on soil P content (ranging around $35\,\mu mol\,m^{-2}\,s^{-1}$, Fig. 5c). This may be due to the large differences between foliar P (Fyllas et al., 2009) and soil P for this specific site (Quesada et al., 2010). The

5 reason for this difference is not clear. The limitation of the linear regression between V_{cmax} and total soil P hypothesis is that it does not reproduce the saturation in V_{cmax} due to high levels of P content. One example of this is the high V_{cmax} value estimated in Cuzco Amazonico (CUZ, Peru) (Fig. 5c) due to the elevated total soil P in this site (Fig. 4). Mercado et al. (2011) have suggested the use of a modified photosynthesis

10 model that includes both P and N limitation of the main photosynthetic parameters, as described in Domingues et al. (2010). More detailed physiological analyses are important for a better definition of the relation between V_{cmax} and the P limitation. There are no clear relationships between SLA and other biophysical properties, therefore we interpolated the site values to the entire basin using the kriging interpolation method

15 (Fig. 5d).

The above-ground wood net primary productivity (NPP_w) field database is used in this work for comparison to the simulated NPP_w. IBIS, like many other ecosystem models, simulates a generic woody biomass pool which does not differentiate between above-ground and belowground components. Therefore, to facilitate comparison with

20 the field data, which is above-ground woody productivity only, the simulated woody net primary productivity was divided by 1.21 to remove the below ground coarse root fraction of the simulated NPP wood in the model as suggested in Houghton et al. (2001). Malhi et al. (2004) present a large data set on above-ground coarse wood productivity in 104 neotropical forest plots, all located at an elevation lower than $1000\,m$, in

25 mixed-age old-growth humid forest, and with no human disturbance. These data are aggregated to the $1° \times 1°$ grid cell resolution for the studied area of this work, representing 25 grid-points across Amazonia available for comparison with our simulation results (Fig. 1, Table 1). There is high productivity in the west and low productivity in

Central and Eastern Amazonia, varying in space from 0.15 up to $0.55\,kg\,C\,m^{-2}\,yr^{-1}$, that represents an overall variability of 260 % (or $0.55/0.15 = 3.6$ times) (Fig. 6a).

Malhi et al. (2006) present a synthesis of data on woody above-ground live biomass of old-growth lowland tropical forest for 227 plots across South America. This data was
5   rescaled to the one-degree grid resolution resulting in 71 sites for comparison with our simulation results (Fig. 1, Table 1). The spatial distribution of biomass shows high biomass in the slow growing Central Amazonia forest and Guyanas, with low biomass in the western faster growing forests and the dryer southern and eastern margins. The observed woody biomass ranges from 9 up to $20\,kg\,C\,m^{-2}$ within the average of plots
10   in a grid cell that represent a spatial variability of 120 % (or $20/9 = 2.2$ times) among forest sites (Fig. 6b).

2.3   Model configuration setup

In order to quantify the response of IBIS to spatially varying parameters based on observed data we performed a suite of simulations in 4 different exercises categories
15   (Table 2). The first category is a simulation over the entire Amazon basin that uses the original configuration of the IBIS model. This simulation serves as a reference to the other experiments and is referred to as the control simulation (CA). The second simulation assumes the original configuration CA but alters the allocation of NPP to wood, foliage and roots so that it is more consistent with observations, allocating one third for
20   each component (34 %, 33 %, 33 % respectively) (SA3a) (Malhi et al., 2011). In these tests, constant parameter values are assigned fixed in space for the entire Amazon basin (homogeneous parameterization). The SA3a simulation was done to be better comparable to field data. The third simulation category referred to as the site-level simulation (SS) tests the importance of using the spatially heterogeneous field data to
25   represent the fundamental parameters. In these simulations the model is run only at the site-level with the parameters from our database (Fig. 5, dots and Table 1). Comparison of these simulations (SS) with CA and SA3a and with observations provides

an understanding of the ability of the model to simulate the productivity and biomass at individual locations. The fourth simulation category uses the basin-wide spatially varying parameter values (Fig. 5, background map and Table 1) derived in this study. The results of this exercise (referred to as RS) when compared to CA, SA3a and the observations, quantify the value of using best estimates of basin-wide parameters to derive productivity and biomass values. The specific parameter values and simulation runs are summarized in Table 2. We considered spatial variation in carbon allocation to wood, leaves and fine roots, woody biomass residence time, maximum carboxylation capacity of Rubisco (V_{cmax}) and specific leaf area (SLA) (Table 2).

The model was forced by prescribed climate based on the Sheffield et al. (2006) database, which is a combination of global observation-based datasets with reanalysis data from the National Center for Environmental Prediction – National Center for Atmospheric Research (NCEP-NCAR). The dataset is available from 1970 to 2008 (39 yr), has one-degree spatial resolution and 3 h time resolution that was linearly interpolated to one hour.

The model simulations were run for a total of 680 yr (1329–2008). The long simulation was required to allow the slow carbon pools to come to equilibrium. There was an initial spin-up of 386 yr (from 1329–1715) under constant pre-industrial atmospheric CO_2 values (278 ppm). The spin-up simulation started from near bare ground until soil carbon, vegetation structure and biomass achieved an equilibrium state. The runs were continued from 1715 up to 2008 with increasing prescribed atmospheric CO_2 concentrations (from 278 to 386 ppm). During the entire 680 yr run the prescribed climate was applied cyclically.

Soil texture data was based on the IGBP-DIS global soil and Quesada et al. (2010) dataset. The control simulation (CA) and regional simulation (RS) uses the regional map of texture while the site level simulations (SS) consider soil texture site level information from Quesada et al. (2010). The soil depth is considered homogeneous with 10 m in all simulations. There are 6 soil layers with thicknesses from the top layer to the bottom of 0.25, 0.375, 0.625, 1.25, 2.5, 5 m depth.

Full Screen / Esc

Printer-friendly Version

Interactive Discussion

No land use changes or other disturbances (e.g. fire) were incorporated in the simulations. Therefore, the results are for potential vegetation conditions (the vegetation in equilibrium with the prescribed soil and climate). Potential vegetation simulations were chosen because they should be most comparable to the field data, which were
5 collected in undisturbed old-growth tropical forest plots

2.4 Statistical analyses

The simulated variables are averaged for the last 10 yr of simulation (1999–2008) and compared to the field data within a grid cell, which represent an average of the period of sampling. Besides the correlation coefficient and linear regression usual to the
10 comparison between data series we use the suggested statistics described in detail by Willmott (1982). We include the index of agreement, which is complementary to the correlation coefficient to verify the level of agreement between two data series (Willmott, 1982). The index of agreement provides information on how correlated and how distant the simulated data points are from the reference (observation) (while the corre-
15 lation coefficient might have a high value just because the data are well correlated but not necessarily are close in absolute values). The index of agreement varies from 0 to 1 where 0 means a very poor agreement and 1 the maximum agreement.

3 Results

3.1 Comparison of simulations and field observations

20 We performed a series of sensitivity analyses with the model and they pointed out the potential factors affecting the spatial variability of IBIS simulated wood productivity and biomass (Supplement A and B). The sensitivity analyses pointed out maximum Rubisco as an important factor that has to be well represented in space to better simulate of NPP_w by the numerical models (Table B). The woody residence time was identi-
25 fied as the most relevant factor for reproducing the spatial variability in above-ground

Amazon Heterogeneity

A. D. de Almeida Castanho et al.

Amazon Heterogeneity

A. D. de Almeida Castanho et al.

biomass in the numerical models (Table B). In this section we quantify the use of the combined effect of all site-specific observed parameter information (SS, Table 2) on simulated productivity and biomass in contrast to the previous homogeneous parameter assumption (CA and SA3a, Table 2). The heterogeneous parameterization simulation results (SS) is compared to observations available for wood productivity and above-ground biomass (Fig. 7).

The control simulation (CA) shows a systematic overestimation of NPP_w when compared to observations (Fig. 7a, dark square). This is mainly because of the assumption of 50 % allocation of carbon to wood. Although many DGVMs use this 50 % allocation rule, carbon allocation measurements in sites across Amazonia show that this assumption is unrealistic and leads to a large bias in simulated wood productivity. When allocation to wood is set to 34 % (SA3a) simulated NPP_w is in better agreement with the average observation values (Fig. 7a, dark triangles).

Similar results are shown for the above-ground biomass comparison (Fig. 7b). The simulated biomass in the control (CA) does not reproduce the spatial variability but average values are similar to those from observations (Fig. 7b, dark square). However the good agreement of biomass with observations in CA simulation is for the wrong reasons since the model parameterizations in CA overestimate the total carbon allocated to wood (woody carbon allocation 50 %) and underestimate τ_w, residence time 25 yr), and these two factors compensate each other. If only one of the parameterizations is corrected, for example carbon allocation (SA3a, dark triangle), the estimated biomass deviates strongly from the observations (Fig. 7b), which is consistent with results with the DVM ORCHIDEE (Delbart et al., 2009).

In summary, the homogenous parameterizations applied in the CA and SA3a experiments are capable of improving mean biomass estimates (sometimes due to compensation of errors). However, as can be noticed in Fig. 7a, b, the homogeneous parameterizations clearly fail to reproduce the spatial variability of observed productivity and biomass. The next results show the combined effect of all heterogeneous parameterizations based on the site-level field observations (Fig. 7, red and black).

The NPP_w analyses are made for two series of data, one with only the series of data points where there are available field estimates of V_{cmax} (Fig. 7a, c, in red), hereinafter Series A. Another data series is defined where the V_{cmax} are extrapolated to all other locations where there are NPP_w measurements available (Table 1), hereinafter Series B (Fig. 7c, in black). The full set of NPP_w that include sites with known V_{cmax} from field and extrapolated V_{cmax} in this work is called Series A + B (Fig. 7c, in red and black). The NPP_w simulation SS with heterogeneous parameterization (Fig. 7a, red circles) shows better agreement with the observations when compared to the previous homogeneous assumption SA3a (Fig. 7a, triangles). The coefficient of correlation improves from 0.10 to 0.71, the regression slope (error) improves from −0.04(0.03) to 0.6(0.2) and intercept (error) from 0.35(0.05) to 0.16(0.07) (Table 3, Series A). The slope coefficient improves but is still low, showing that the NPP_w from locations with low observed values is overestimated by the model (Fig. 7a). The NPP_w simulated by IBIS with the new spatial parameterization better reproduces the observed spatial variability as confirmed by the high values of the index of agreement (Fig. 7a, Table 3); from 0 (SA3a Series A) to 0.7 (SS Series A). In summary it showed improved agreement between simulations and observations when heterogeneous observations-based parameterizations are used compared to the simulations with homogenous parameters (Table 3, Series A).

The comparison of the extrapolated parameterization is done in Series B (Table 3, Fig. 7c in black only). The comparison of results of Series B in simulation RS with SA3a shows that some simulations are closer to the observations (index of agreement 0.4 compared to 0.3) but is not better correlated (correlation coefficient 0.66 compared to 0.79). This means that, as expected, the procedure for regionalization of parameter data is not as good as field estimates. However the conclusions for the regionalization of NPP_w are still limited to a validation against only 10 data points that are not representative of the entire basin.

Similar to NPP_w, AGB_w comparisons were made for two series: one with only the data points where woody residence time estimates are known (Fig. 7b, in red) referred

to as Series C; another data series is defined where the woody residence time is extrapolated to all other AGB_w data collection points, called Series D (Fig. 7d, in black). The full set of simulated AGB_w values derived from both direct measurements of residence time and the extrapolatoins, is called Series C + D (Fig. 7d, in red and black). The heterogeneous woody residence time data has the strongest influence on simulated AGB_w spatial variability (Fig. 7b, red circles). The data series SS captures the spatial variability of the AGB_w much better than the SA3a simulation with homogeneous parameterizations (dark triangles). The coefficient of correlation of simulated woody above-ground biomass improves from 0.22 with homogeneous parameterization (SA3a, Series C) to 0.80 with spatial varying parameters (SS, Series C). The regression analyses shows a significant improvement of the slope(error) from 0.05(0.05) to 1.06(0.18), and intercept(error) from 6.5(0.8) to −2.8 (2.8) (Table 4, Series C). The index of agreement in Series C improved from 0 with homogeneous parameterization (Table 4, Series C, SA3a) to 0.8 with heterogeneous parameterization (Table 4, Series C, SS). Some outliers were identifyed and are discussed in detail in the Supplement D.

The statistical analyses of AGB_w from Series D (with the extrapolated woody residence time) provides a measure of the value of extrapolation adopted in this work (Table 4, Series D). The results shows improvement on all statistical parameters comparing the regional simulation (RS, Series D) to the homogeneous assumption (SA3a, Series D). The correlation coefficient improved from −0.006 to 0.52 and the index of agreement from 0 to 0.6. As expected, the results derived from extrapolated parameters (RS, Series D) are in poorer agreement with the results derived from SS-Series C where residence time is site measured, with a lower slope (0.44) and intercept of 6.9 and larger variance of the distribution differences (6.5 compared to 3.3 in Series C).

3.2 Regional simulation analyses (RS)

In this section we present the basin-wide simulated woody above-ground productivity and biomass (simulation RS), based on our maps of spatially varying parameters (Table 1, Fig. 5). Quantitative validation of simulated NPP_w and AGB_w was discussed in

Title Page

Abstract | Introduction

Conclusions | References

Tables | Figures

⏮ | ⏭

◀ | ▶

Back | Close

Full Screen / Esc

Printer-friendly Version

Interactive Discussion

Sect. 3.1 (Table 3, Series B, Table 4, Series D) at the specific locations in the basin. Qualitatively, analyzing the simulation for the entire basin there is much greater spatial variation of the NPP_w and AGB_w in the RS simulation (Fig. 8c, d) compared to CA (Fig. 8a, b).

⁵ The NPP_w RS map (Fig. 8c) follows the spatial variability given by the soil total phosphorus map (Fig. 4). There is higher productivity in the west where the fertility is higher and also in Central West Amazonia where P content is higher and the soil is silt. The productivity decreases in Central and East Amazonia and increases again in the northeast of the region. There is a low region of NPP_w in the north of Brazil

¹⁰ and south of Venezuela due to the low estimated soil fertility in that area. A qualitative comparison of this simulation with published satellite derived map of NPP in Amazonia (Nunes et al., 2012) seems to reproduce similar spatial variability. A detailed analysis of the comparison of these simulations including land use change and other disturbances and comparison with satellite products is in progress (Castanho et al., 2012).

¹⁵ The biomass map shows the pattern observed from field data with the west to east trend of higher biomass in Central and North Eastern Amazonia (RS, Fig. 8d). The increased spatial variability is governed by the woody residence time map. The biomass map (Fig. 8d) can be compared to the estimated biomass map from Malhi et al. (2006). There is relatively good agreement of higher biomass covering the central and extend-

²⁰ ing to the northeast of Amazonia forest. In the observed data set the highest biomass values in the Central Amazon are clustered around the sites of measurement, which is most likely an effect of extrapolation from the few data points available (Malhi et al., 2006). There is an agreement between both maps, with lower biomass in the west and south. The gradient of biomass in the transition to the "cerrado" region diverges in the

²⁵ absolute values from the observational estimates. This is a region where there are few field data, which makes the validation difficult.

4   Discussion and Conclusions

1. Homogeneous parameterizations and climate alone do not capture the spatial variability of woody above-ground productivity (NPP$_w$) and biomass (AGB$_w$) present in the field data.

The model homogeneous parameterization simulation driven by climate and soil physical (water) properties does not capture the observed spatial variability of NPP$_w$ (260 %, the highest value is 3.6 times higher than the lowest value, Malhi et al., 2004) and AGB$_w$ (120 % highest value is 2.2 times higher than the lowest value, Malhi et al., 2006) across the Amazon basin (Fig. 7a, b dark square).

The spatial scale and diverse topography of the Amazonian basin allows a large variability of climatological scenarios for a single tropical forest. However, field data analyses have shown poor correlation between climate variables and large-scale variation of productivity and biomass patterns in the basin (Malhi et al., 2004; Quesada et al., 2012; Galbraith et al., 2012). In analyses of spatial patterns of productivity, Malhi et al., (2004) found no obvious relationship between the spatial distribution of wood productivity and precipitation, dry season length, or radiation, but the authors did find some decline in woody productivity with increasing temperature. However, the lower temperature in the Western Amazonia is indirectly correlated to the higher soil fertility in that region, making it difficult to directly correlate temperature and productivity given the strong correlation between productivity and soil fertility. In analyses of basal area spatial patterns Malhi et al. (2006) found some correlation with dry season length and precipitation. The decline in basal area however was evident only in extreme water stress for longer dry season length (more than 4 months).

In this study we found that, for IBIS, the spatial variation of climate in the Amazon basin imparts productivity and biomass variation of 35 % and 45 % from the basin minimum (Table B). IBIS and most numerical models underestimate or do not explicitly consider mortality rates due to short or long term disturbances due to temperature extremes, drought or flooding (Phillips et al., 2010; Galbraith et al., 2012). However,

because the observed data were collected at sites specifically chosen to be free of recent disturbance, lack of climate-stress mortality is not a factor in the simulated low sensitivity to climate variation. Therefore, the low variability by climate in the IBIS simulations appears to be a robust indication of the scale of the actual variability imparted
5 by climate.

2. Maximum carboxylation capacity of Rubisco activity (V_{cmax}) as a function of soil fertility is the primary variable controlling the simulated variation of woody above-ground productivity across the Amazon.

Observations suggest that soil fertility plays an important role in creating spatial vari-
10 ation of productivity across the Amazon basin but little is known about the specific pathways (Quesada et al., 2012; Aragão et al., 2009, Malhi et al., 2004). Some of the possible factors that have been explored are for example differences in gross primary productivity, respiration rates, and carbon allocation between carbon pools.
　　Malhi et al. (2004) suggest that carbon allocation may alternatively be related
15 to the spatial variability of NPP_w, due to shifts in allocation to roots in less fertile soils. Alternatively the authors data analyses also suggest that carbon use efficiency (CUE = NPP/GPP) is higher in the west, that means that beside a potential higher GPP in the higher fertility soils western region there is also a potential higher autotrophic respiration rates in the lower fertility soils of Central Amazonia. We found that changes in
20 GPP and autotrophic respiration imparted by changes in leaf photosynthetic capacity (related to maximum carboxylase capacity of Rubisco) is the strongest candidate to explain the spatial variability of productivity. The sensitivity tests show that a spatial variability in Rubisco (from 75–40 μmol CO_2 m^{-2} s^{-1}, SA5, Table A) leads to simulated change in NPP_w of 60–80 % (Table B). A shift in woody carbon allocation from 50 %
25 to 25 % imparts a change of 60 % in NPP_w (Table B). Our analyses suggest that V_{cmax} driven by soil fertility plays a stronger role than carbon allocation in the spatial variability of NPP_w.

Amazon Heterogeneity

A. D. de Almeida Castanho et al.

Title Page

Abstract　　Introduction

Conclusions　　References

Tables　　Figures

◄　　►

Back　　Close

Full Screen / Esc

Printer-friendly Version

Interactive Discussion

3. Heterogeneous parameterizations of key biophysical properties based on site specific data improves the simulated woody above-ground productivity compared to homogeneous parameterizations.

Based on the established correlation between V_{cmax} and leaf P content (Mercado et al., 2009; Mercado et al., 2011), and knowing that leaf nutrients are directly related to soil nutrients (Fyllas et al., 2009), we estimated the maximum carboxylation capacity of Rubisco scaled according to site observed total soil P from Quesada et al. (2010). The spatial heterogeneity of other parameters of minor effect in the NPP_w calculation, such as carbon allocation, residence time, and specific leaf area were also obtained based on published site field data. The simulated NPP_w with IBIS numerical model using heterogeneous parameterization was compared to NPP_w field data (Malhi et al., 2004).

As presented in the Results (Sect. 3) the use of heterogeneous parameterizations in IBIS based on field data significantly improved the simulation of NPP_w (correlation coefficient −0.1 to 0.71, respectively for the homogeneous and heterogeneous parameterization, Table 3). The simulated NPP_w values at the lower end of the observations were not well captured by the model as indicated by a slope of 0.58 ± 0.20 and an offset of 0.16 ± 0.07 (Table 3). This could be due to an overestimation of the V_{cmax} for low fertility sites or by other factors that are not captured by the model. For example, lowland areas may have higher respiration rates than what the model predicts, due to the higher temperatures and/or the higher respiratory costs due to slower growing plants in less fertile soils (Malhi et al., 2004). These effects may not be fully represented in IBIS and may contribute to the overestimation of the low end of NPP_w, in Central and East Amazonian sites. A detailed analyses of field data information on the respiration rates, available biomass in decomposition state and how the model reproduce these processes needs to be carefully addressed in the future. A factor that may be contributing to a general overestimation of NPP_w is the simulated LAI. The LAI in the model is systematically higher than the observations, which would cause an increase in simulated NPP. The exaggerated increase in the LAI in time is a response to increasing

Full Screen / Esc

Printer-friendly Version

Interactive Discussion

atmospheric CO_2. Each year there is more carbon to allocate and the allocation in the model is constant in time as is the residence time of the leaves. Therefore, the LAI in the model increases with time. The assumption of constant allocation and residence time is probably too simplistic but the right balance of changes in carbon allocation between the plant components in space and time is poorly known.

In our analyses we observed that the difference of simulated NPP_w from the observations do not appear to be related to misrepresentation of carbon allocation. For example, if we define woody carbon allocation to a value that minimizes the NPP_w error then the carbon allocation to wood would have to be unrealistically low (between 0.15–0.25 compared to the observed values 0.25–0.5). Therefore, there are most likely other unknown factors contributing to the lack of good agreement, including shorter time-scale variability of parameter response to drought, fertility and disturbance for which we do not yet have data. Further improvements of these parameters are clearly required and are discussed in suggestion for future work below.

4. Woody residence time is the most important mechanism affecting the magnitude and spatial distribution of simulated AGB_w.

Our results of the IBIS sensitivity analyses agree with the analyses of Senna et al. (2009) and Delbart et al. (2010) suggesting that woody residence time is the most important mechanism affecting the magnitude and spatial distribution of simulated AGB_w. Results from IBIS simulations show that with a spatial variation of woody residence time within the range of 25 to 100 yr, AGB_w changes by 180 % from the basin minimum (Table B).

5. Heterogeneous parameterizations of key biophysical properties based on site specific data improves the simulated woody above-ground biomass when compared to homogeneous parameterizations.

Given the importance of the woody residence time in the simulated AGB_w, we used field data available for 21 sites across the Amazon basin to represent the spatial heterogeneity of woody residence time (Phillips et al., 2004; Galbraith et al., 2012). The

spatial variability of other parameters of minor effect in AGB_w as carbon allocation, V_{cmax}, and specific leaf area index were also included in the simulation of AGB in the model.

The comparison of the simulated AGB_w with observation showed an improvement in coefficient of correlation from 0.22 in the homogeneous experiments (SA3a) to 0.80 in the heterogeneous ones (SS) (Table 4). The regression fit is much closer to the 1 : 1 relation. The good agreement comes from two factors, one is that the AGB simulated by the model was based on residence times from field data, the other one is that most of the sites for comparisons of biomass come from direct measurement of individual trees (Baker et al., 2004b). So both model and field measurement methodologies used the most accurate information available.

6. The regional maps of key parameter values developed in this study significantly improve simulated AGB_w compared to simulations using homogeneous parameterization assumptions.

The quality of the upscaled maps of the physiological properties depends on two factors: (1) the number of site level data points available and how representative these sites are of the larger scale; and (2) how well we understand what drives the spatial variability of these properties. Unfortunately there are relatively few field data sites (Table 1) and the processes that govern the spatial variability are not completely understood, which makes our upscaling exercise somewhat speculative. We developed a set of extrapolations of the observed field data to the entire Amazon basin in order to obtain greater heterogeneity in the simulations of NPP_w and AGB_w.

The V_{cmax} was extrapolated to the entire basing using a soil map of P and the regression equation between field based V_{cmax} and P (Table 1, Fig. 5c). The comparison of simulated NPP_w (with the extrapolated V_{cmax}) with observation was represented by a few location points ($n = 9$). Although the simulation results for some of the individual data points were improved, it was not significant ($p > 0.5$) considering the small size of the sample.

We estimated woody residence time for the entire basin based on a simple kriging interpolation (Fig. 5b). The large scale spatial variability appears to be well defined, showing a trend of higher turnover rate in the west then in the Central East Amazonia, that is in qualitative agreement with the observations. The comparison of the basin-wide simulations suggests that this first attempt at spatially varying biophysical parameters improves the simulations. For example, the coefficient of correlation of simulated AGB_w with observations at 46 locations increased (0.52, RS) compared to the more standard homogeneous parameters (~ 0, CA) (Table 4). The results show that the proposed map of woody residence time, despite its uncertainties, is a better option than a homogeneous assumption for the entire basin.

Giving the importance of the residence time in simulating the AGB_w it is fundamental to understand the factors that govern the spatial distribution of woody residence time. However there is no single mechanism that is known to control geographic patterns of it. Many authors have explored this topic including Quesada et al. (2012) who have argued that stem turnover is correlated with soil physical properties such as soil depth, soil structure and topography. However, residence time has also been found to be well correlated with soil fertility within the Amazon (Phillips et al., 2004; Galbraith et al., 2012). There are several physically adverse soil conditions, such as rooting depth limitations, low drainage capacity, poor soil structure, topography position, that might affect woody residence time and are difficult to account for (Quesada et al., 2012). Delbart et al. (2010) presented an alternative solution of dynamic estimation of woody residence time as a function of NPP, whereby the function was defined based on the empirical correlation between them. This NPP based assumption is however only valid for a forest in equilibrium and the NPP needs to be well estimated by the model. This combination of poorly known governing factors makes it difficult to mechanistically determine residence time across the Amazon. We believe that our prescribed approach using a simplified interpolation (of woody residence time) of the site level data is a good starting point to address the spatial variability, although we cannot asume residence times will be remain unchanged under current future scenarios of atmospheric change.

7. Simulated total live above-ground biomass (73 PgC) is comparable to the mean of published estimates.

One of the main goals in improving model representation of net primary productivity, residence time, carbon allocation, and photosynthetic capacity is to provide greater confidence of biomass estimates in the Amazon. Based on the simulated above-ground biomass in this work, we estimate the corresponding total above-ground biomass carbon content (T_{AGB}) in the Amazon basin. The T_{AGB} for an area of 5.65×10^6 km^2 of forest in our control run (CA) and final regional heterogeneous parameterization simulation (RS) differed by only about 3 %, with 71 PgC and 73 PgC, respectively. The difference is not large in the regional total but is significant in the spatial distribution across the basin, as presented in the regional simulation section (Fig. 8).

We compare our simulated T_{AGB} to estimates derived from four published studies. Exact comparison is difficult because the areas of summation, methodologies and assumptions vary among the estimates. For example, the IBIS simulated values and the Malhi et al. (2006) forest inventory estimates are based on old growth forest biomass only, while the satellite based estimates e.g. (Saatchi et al., 2011; Baccini et al., 2012) explicitly include disturbed forests, secondary forests and different thresholds in the tree cover fraction are assumed. As a result, the satellite estimates will be less than the estimates derived from models or native forest inventories. Despite these differences a comparison is qualitatively instructive (Fig. 9). The seven estimates of above-ground biomass presented by Houghton et al. (2001) scaled to our area of study 5.65×10^6 km^2 give a range of 42–100 PgC (Fig. 9). Malhi et al., (2006) estimate T_{AGB} (rescaled to our studied area of 5.65×10^6 km^2) of 89–92 PgC (including trees less than < 10 cm dbh and lianas). The two new satellite estimates of biomass are 68 PgC (Baccini et al., 2012) and 54 PgC (Saatchi et al., 2011) in an equivalent area of 5.65×10^6 km^2. The IBIS simulated T_{AGB} is greater than the satellite based values which include disturbances and less than the Malhi et al. (2006), which are for old-growth undisturbed forests only.

Title Page

Abstract | Introduction

Conclusions | References

Tables | Figures

|◄ | ►|

◄ | ►

Back | Close

Full Screen / Esc

Printer-friendly Version

Interactive Discussion

8. Further improvement of regional simulations is limited by lack of data.

Our exercise in up-scaling the sparse site-specific data to the entire Amazon basin improved the simulations compared to heterogeneous simulations. However, accurate regional simulation is still limited by data scarcity of field data information.

The improvement in the upscaling method could be achieved in the future by:

1. Expanding the network of field data monitoring to a better characterization of the basin. Given the new knowledge that the current field sites have provided, an expansion of the field network to strategic representative locations could bring more clarity to extrapolation methods of forest biophysical properties. As for example measures of soil P in Central Amazonia. The soil P extrapolations would suggest that as a region rich in P and that would affect significantly the productivity in that region as a result of our analyses.

2. Better understanding of the physiological processes that govern the spatial variability of the main parameterizations. Some progress has been made in respect to better understanding the different forest physiological processes, as for example the relation between V_{cmax} and Phosphorus or other nutrients in leaves (Malhi et al., 2009; Fyllas et al., 2009; Domingues et al., 2005). These finding were crucial to our estimates of V_{cmax} in space, but more information on how Phosphorus is distributed across the region would also be important. Our results showed also the importance of the woody residence time on the simulation of the AGB_w in space. A fuller understanding of what causes the residence time variability in space is essential to an accurate simulation of biomass across the basin. It is also necessary to better understand the allocation of carbon to wood, leaves and roots, as the current data base is very limited in space.

3. Developing new satellite and airborne measurements of key biophysical properties and mechanisms. The Amazon forest is large and heterogeneous, thus satellite and airborne measurement are very useful to help characterize the large areas

complementary to field data. The Carnegie Airborne Observatory (CAO), that has been remotely monitoring tropical canopy chemistry, diversity and structure (Asner et al., 2010), uses a combination of LiDAR and spectrometer that are able to characterize large areas with high spatial resolution. This technology would be able to characterize the P content in leaves and therefore the Rubisco capacity of the vegetation across large spatial scales, besides total above ground biomass estimates.

4. Improving model physical processes. For example, photosynthetic response to nutrient limitation is an important factor determining biomass productivity however most DGVM's do not include it. Tree mortality as a function of drought stress is another important process not considered in most models.

5. Including land use change from deforestation and fire in the simulation is an important next step. This would facilitate comparison with satellite products of biomass and a validation of biomass spatial variability simulated by the model (Baccini et al., 2012; Saatchi et al., 2011).

6. A final area of improvement is the representation of the temporal variability of fundamental parameters. Field studies have shown that the Amazonian forest is not only spatially heterogeneous but also temporally dynamic (Phillips et al., 2004; Chave et al., 2010). Changes in structure, dynamics and composition of the forest are not restricted to specific local events but respond to long-acting and widespread environmental stimulations. The IBIS dynamic vegetation model, as with most other models, could represent time-varying dynamics of properties that are currently constant in time (e.g. Rubisco, residence time, carbon allocation) but appropriate data are required.

Supplementary material related to this article is available online at: http://www.biogeosciences-discuss.net/9/11767/2012/ bgd-9-11767-2012-supplement.pdf.

References

Aragão, L. E. O. C., Malhi, Y., Metcalfe, D. B., Silva-Espejo, J. E., Jiménez, E., Navarrete, D., Almeida, S., Costa, A. C. L., Salinas, N., Phillips, O. L., Anderson, L. O., Alvarez, E., Baker, T. R., Goncalvez, P. H., Huamán-Ovalle, J., Mamani-Solórzano, M., Meir, P., Monteagudo, A., Patiño, S., Peñuela, M. C., Prieto, A., Quesada, C. A., Rozas-Dávila, A., Rudas, A., Silva Jr., J. A., and Vásquez, R.: Above- and below-ground net primary productivity across ten Amazonian forests on contrasting soils, Biogeosciences, 6, 2759–2778, doi:10.5194/bg-6-2759-2009, 2009.

Asner, G. P., Powell, G. V. N., Mascaro, J., Knapp, D. E., Clark, J. K., Jacobson, J., Kennedy-Bowdoin, T., Balaji, A., Paez-Acosta, G., Victoria, E., Secada, L., Valqui, M., and Hughes, R. F.: High-resolution forest carbon stocks and emissions in the Amazon, Proc. Natl. Acad. Sci., 107, 16738–16742, doi:10.1073/pnas.1004875107, 2010.

Baccini, A., Goetz, S. J., Walker, W. S., Laporte, N. T., Sun, M., Sulla-Menashe, D., Hackler, J., Beck, P. S. A., Dubayah, R., Friedl, M. A., Samanta, S., and Houghton, R. A.: Estimated carbon dioxide emissions from tropical deforestation improved by carbon-density maps, Nat. Clim. Change, 2, 182–185, 2012.

Baker, T. R., Phillips, O. L., Malhi, Y., Almeida, S., Arroyo, L., Di Fiore, A., Erwin, T., Higuchi, N., Killeen, T. J., Laurance, S. G., Laurance, W. F., Lewis, S. L., Monteagudo, A., Neill, D. A., Núñez Vargas, P., Pitman, N. C. A., Silva, J. N. M., and Vásquez Martínez, R.: Increasing biomass in Amazonian forest plots, Philos. T. Roy. Soc. B, 359, 353–365, doi:10.1098/rstb.2003.1422, 2004a.

Baker, T. R., Phillips, O. L., Malhi, Y., Almeida, S., Arroyo, L., Di Fiore, A., Erwin, T., Killeen, T. J., Laurance, S. G., Laurance, W. F., Lewis, S. L., Lloyd, J., Monteagudo, A., Neill, D. A., Patiño, S., Pitman, N. C. A. M., Silva, J. N., and Vásquez Martínez, R.: Variation in wood

Amazon Heterogeneity

A. D. de Almeida Castanho et al.

Title Page

Abstract	Introduction
Conclusions	References
Tables	Figures

◄◄	►►
◄	►
Back	Close

Full Screen / Esc

Printer-friendly Version

Interactive Discussion

density determines spatial patterns in Amazonian forest biomass, Glob. Change Biol., 10, 545–562, doi:10.1111/j.1365-2486.2004.00751.x, 2004b.

Chave, J., Navarrete, D., Almeida, S., Álvarez, E., Aragão, L. E. O. C., Bonal, D., Châtelet, P., Silva-Espejo, J. E., Goret, J.-Y., von Hildebrand, P., Jiménez, E., Patiño, S., Peñuela, M. C., Phillips, O. L., Stevenson, P., and Malhi, Y.: Regional and seasonal patterns of litterfall in tropical South America, Biogeosciences, 7, 43–55, doi:10.5194/bg-7-43-2010, 2010.

Coe, M. T., Costa, M. H., and Howard, E. A.: Simulating the surface waters of the Amazon River basin: impacts of new river geomorphic and flow parameterizations, Hydrol. Process., 22, 2542–2553, doi:10.1002/hyp.6850, 2008.

Davidson, E. A., De Araujo, A. C., Artaxo, P., Balch, J. K., Brown, I. F., C. Bustamante, M. M., Coe, M. T., Defries, R. S., Keller, M., Longo, M., Munger, J. W., Schroeder, W., Soares-Filho, B. S., Souza, C. M., and Wofsy, S. C.: The Amazon basin in transition, Nature, 481, 321–328, 2012.

Delbart, N., Ciais, P., Chave, J., Viovy, N., Malhi, Y., and Le Toan, T.: Mortality as a key driver of the spatial distribution of aboveground biomass in Amazonian forest: results from a dynamic vegetation model, Biogeosciences, 7, 3027–3039, doi:10.5194/bg-7-3027-2010, 2010.

Delire, C. and Foley, J. A.: Evaluating the performance of a land surface/ecosystem model with biophysical measurements from contrasting environments, J. Geophys. Res.-Atmos., 104, 16895–16909, 1999.

Domingues, T. F., Berry, J. A., Martinelli, L. A., Ometto, J. P. H. B., and Ehleringer, J. R.: Parameterization of canopy structure and leaf-level gas exchange for an Eastern Amazonian tropical rain forest (Tapajós National Forest, Pará, Brazil), Earth Interact., 9, 1–23, doi:10.1175/ei149.1, 2005.

Domingues, T. F., Meir, P., Feldpausch, T. R., Saiz, G., Veenendaal, E. M., Schrodt, F., Bird, M., Djagbletey, G., Hien, F., Compaore, H., Diallo, A., Grace, J., and Lloyd, J. O. N.: Co-limitation of photosynthetic capacity by nitrogen and phosphorus in West Africa woodlands, Plant Cell Environ., 33, 959–980, doi:10.1111/j.1365-3040.2010.02119.x, 2010.

Eva, H. D., Huber, O., Achard, F., Balslev, H., Beck, S., Behling, H., Belward, A. S., Beuchle, R., Cleef, A., Colchester, M., Muller, J. M., Pereira., J. M., Peres, C., Prance, G. T., Roberts, J. M., and Salo, J.: A proposal for defining the geographical boundaries of Amazonia, Report, European Communities, Luxembourg, 2005.

Feldpausch, T. R., Banin, L., Phillips, O. L., Baker, T. R., Lewis, S. L., Quesada, C. A., Affum-Baffoe, K., Arets, E. J. M. M., Berry, N. J., Bird, M., Brondizio, E. S., de Camargo, P.,

Title Page

Abstract | Introduction

Conclusions | References

Tables | Figures

|◄ | ►|

◄ | ►

Back | Close

Full Screen / Esc

Printer-friendly Version

Interactive Discussion

Chave, J., Djagbletey, G., Domingues, T. F., Drescher, M., Fearnside, P. M., França, M. B., Fyllas, N. M., Lopez-Gonzalez, G., Hladik, A., Higuchi, N., Hunter, M. O., Iida, Y., Salim, K. A., Kassim, A. R., Keller, M., Kemp, J., King, D. A., Lovett, J. C., Marimon, B. S., Marimon-Junior, B. H., Lenza, E., Marshall, A. R., Metcalfe, D. J., Mitchard, E. T. A., Moran, E. F., Nelson, B. W., Nilus, R., Nogueira, E. M., Palace, M., Patiño, S., Peh, K. S.-H., Raventos, M. T., Reitsma, J. M., Saiz, G., Schrodt, F., Sonké, B., Taedoumg, H. E., Tan, S., White, L., Wöll, H., and Lloyd, J.: Height-diameter allometry of tropical forest trees, Biogeosciences, 8, 1081–1106, doi:10.5194/bg-8-1081-2011, 2011.

Foley, J. A., Prentice, I. C., Ramankutty, N., Levis, S., Pollard, D., Sitch, S., and Haxeltine, A.: An integrated biosphere model of land surface processes, terrestrial carbon balance, and vegetation dynamics, Global Biogeochem. Cy., 10, 603–628, 1996.

Foley, J. A., Botta, A., Coe, M. T., and Costa, M. H.: El Nino-Southern Oscillation and the climate, ecosystems and rivers of Amazonia, Global Biogeochem. Cy., 16, 1132, doi:10.1029/2002GB001872, 2002.

Fyllas, N. M., Patiño, S., Baker, T. R., Bielefeld Nardoto, G., Martinelli, L. A., Quesada, C. A., Paiva, R., Schwarz, M., Horna, V., Mercado, L. M., Santos, A., Arroyo, L., Jiménez, E. M., Luizão, F. J., Neill, D. A., Silva, N., Prieto, A., Rudas, A., Silviera, M., Vieira, I. C. G., Lopez-Gonzalez, G., Malhi, Y., Phillips, O. L., and Lloyd, J.: Basin-wide variations in foliar properties of Amazonian forest: phylogeny, soils and climate, Biogeosciences, 6, 2677–2708, doi:10.5194/bg-6-2677-2009, 2009.

Fyllas, N. M., Quesada, C. A., and Lloyd, J.: Deriving plant functional types for Amazonian forests for use in vegetation dynamics models, Perspect. Plant Ecol. 14, 97–110, doi:10.1016/j.ppees.2011.11.001, 2012.

Galbraith, D., Malhi, Y., Castanho, A. D. A., Quesada, C. A., Doughty, C. E., Peh, K. S. H., Affum-Boe, K., Lewis, S., Sonke, B., Phillips, O. L., Lloyd, J., and Fisher, R. A.: The residence time of woody biomass in tropical forests, Plant Ecol. Divers.,in press, 2012,

Green, W. H. and Ampt, G. A.: Studies on soil physics, 1. The flow of air and water through soils, J. Agricult. Sci., 4, 11–24, 1911.

Higgins, M. A., Ruokolainen, K., Tuomisto, H., Llerena, N., Cardenas, G., Phillips, O. L., Vásquez, R., and Räsänen, M.: Geological control of floristic composition in Amazonian forests, J. Biogeogr., 38, 2136–2149, doi:10.1111/j.1365-2699.2011.02585.x, 2011.

Amazon Heterogeneity

A. D. de Almeida Castanho et al.

Title Page

Abstract | Introduction

Conclusions | References

Tables | Figures

◄ | ►►

◄ | ►

Back | Close

Full Screen / Esc

Printer-friendly Version

Interactive Discussion

Houghton, R. A., Lawrence, K. T., Hackler, J. L., and Brown, S.: The spatial distribution of forest biomass in the Brazilian Amazon: a comparison of estimates, Glob. Change Biol., 7, 731–746, doi:10.1111/j.1365-2486.2001.00426.x, 2001.

Kucharik, C. J., Foley, J. A., Delire, C., Fisher, V. A., Coe, M. T., Lenters, J. D., Young-Molling, C., Ramankutty, N., Norman, J. M., and Gower, S. T.: Testing the performance of a dynamic global ecosystem model: water balance, carbon balance, and vegetation structure, Global Biogeochem. Cy., 14, 795–825, doi:10.1029/1999gb001138, 2000.

Li, K. Y., Coe, M. T., and Ramankutty, N.: Investigation of hydrological variability in west africa using land surface models, J. Climate, 18, 3173–3188, 2005.

Li, K. Y., De Jong, R., Coe, M. T., and Ramankutty, N.: Root-water-uptake based upon a new water stress reduction and an asymptotic root distribution function, Earth Interact., 10, 1–22, 2006.

Lloyd, J., Patiño, S., Paiva, R. Q., Nardoto, G. B., Quesada, C. A., Santos, A. J. B., Baker, T. R., Brand, W. A., Hilke, I., Gielmann, H., Raessler, M., Luizão, F. J., Martinelli, L. A., and Mercado, L. M.: Optimisation of photosynthetic carbon gain and within-canopy gradients of associated foliar traits for Amazon forest trees, Biogeosciences, 7, 1833–1859, doi:10.5194/bg-7-1833-2010, 2010.

Malhi, Y.: The carbon balance of tropical forest regions, 1990–2005, Curr. Opin. Environ. Sustain., 2, 237–244, doi:10.1016/j.cosust.2010.08.002, 2010.

Malhi, Y.: The productivity, metabolism and carbon cycle of tropical forest vegetation, J. Ecol., 100, 65–75, doi:10.1111/j.1365-2745.2011.01916.x, 2012.

Malhi, Y., Phillips, O. L., Lloyd, J., Baker, T., Wright, J., Almeida, S., Arroyo, L., Frederiksen, T., Grace, J., Higuchi, N., Killeen, T., Laurance, W. F., Leaño, C., Lewis, S., Meir, P., Monteagudo, A., Neill, D., Núñez Vargas, P., Panfil, S. N., Patiño, S., Pitman, N., Quesada, C. A., Rudas-Ll, A., Salomão, R., Saleska, S., Silva, N., Silveira, M., Sombroek, W. G., Valencia, R., Vásquez Martínez, R., Vieira, I. C. G., and Vinceti, B.: An international network to monitor the structure, composition and dynamics of Amazonian forests (RAINFOR), J. Veg. Sci., 13, 439–450, doi:10.1111/j.1654-1103.2002.tb02068.x, 2002.

Malhi, Y., Baker, T. R., Phillips, O. L., Almeida, S., Alvarez, E., Arroyo, L., Chave, J., Czimczik, C. I., Fiore, A. D., Higuchi, N., Killeen, T. J., Laurance, S. G., Laurance, W. F., Lewis, S. L., Montoya, L. M. M., Monteagudo, A., Neill, D. A., Vargas, P. N., Patiño, S., Pitman, N. C. A., Quesada, C. A., Salomão, R., Silva, J. N. M., Lezama, A. T., Martínez, R. V., Terborgh, J., Vinceti, B., and Lloyd, J.: The above-ground coarse wood productivity

of 104 Neotropical forest plots, Glob. Change Biol., 10, 563–591, doi:10.1111/j.1529-8817.2003.00778.x, 2004.

Malhi, Y., Wood, D., Baker, T. R., Wright, J., Phillips, O. L., Cochrane, T., Meir, P., Chave, J., Almeida, S., Arroyo, L., Higuchi, N., Killeen, T. J., Laurance, S. G., Laurance, W. F., Lewis, S. L., Monteagudo, A., Neill, D. A., Vargas, P. N., Pitman, N. C. A., Quesada, C. A., Salomão, R., Silva, J. N. M., Lezama, A. T., Terborgh, J., Martínez, R. V., and Vinceti, B.: The regional variation of aboveground live biomass in old-growth Amazonian forests, Glob. Change Biol., 12, 1107–1138, doi:10.1111/j.1365-2486.2006.01120.x, 2006.

Malhi, Y., Aragão, L. E. O. C., Metcalfe, D. B., Paiva, R., Quesada, C. A., Almeida, S., Anderson, L., Brando, P., Chambers, J. Q., Da Costa, A. C. L., Hutyra, L. R., Oliveira, P., Patiño, S., Pyle, E. H., Robertson, A. L., and Teixeira, L. M.: Comprehensive assessment of carbon productivity, allocation and storage in three Amazonian forests, Glob. Change Biol., 15, 1255–1274, doi:10.1111/j.1365-2486.2008.01780.x, 2009.

Malhi, Y., Doughty, C., and Galbraith, D.: The allocation of ecosystem net primary productivity in tropical forests, Philos. T. Roy. Soc. B, 366, 3225–3245, doi:10.1098/rstb.2011.0062, 2011.

Mercado, L. M., Lloyd, J., Dolman, A. J., Sitch, S., and Patiño, S.: Modelling basin-wide variations in Amazon forest productivity – Part 1: Model calibration, evaluation and upscaling functions for canopy photosynthesis, Biogeosciences, 6, 1247–1272, doi:10.5194/bg-6-1247-2009, 2009.

Mercado, L. M., Patiño, S., Domingues, T. F., Fyllas, N. M., Weedon, G. P., Sitch, S., Quesada, C. A., Phillips, O. L., Aragão, L. E. O. C., Malhi, Y., Dolman, A. J., Restrepo-Coupe, N., Saleska, S. R., Baker, T. R., Almeida, S., Higuchi, N., and Lloyd, J.: Variations in Amazon forest productivity correlated with foliar nutrients and modelled rates of photosynthetic carbon supply, Philos. T. Roy. Soc. B, 366, 3316–3329, doi:10.1098/rstb.2011.0045, 2011.

Nunes, E. L., Costa, M. H., Malhado, A. C. M., Dias, L. C. P., Vieira, S. A., Pinto, L. B., and Ladle, R. J.: Monitoring carbon assimilation in South America's tropical forests: Model specification and application to the Amazonian droughts of 2005 and 2010, Remote Sens. Environ., 117, 449–463, doi:10.1016/j.rse.2011.10.022, 2012.

Pan, Y., Birdsey, R. A., Fang, J., Houghton, R., Kauppi, P. E., Kurz, W. A., Phillips, O. L., Shvidenko, A., Lewis, S. L., Canadell, J. G., Ciais, P., Jackson, R. B., Pacala, S. W., Mcguire, A. D., Piao, S., Rautiainen, A., Sitch, S., and Hayes, D.: A large and persistent carbon sink in the World's forests, Science, 333, 988–993, doi:10.1126/science.1201609, 2011.

Title Page

Abstract | Introduction

Conclusions | References

Tables | Figures

|◄ | ►|

◄ | ►

Back | Close

Full Screen / Esc

Printer-friendly Version

Interactive Discussion

Peacock, J., Baker, T. R., Lewis, S. L., Lopez-Gonzalez, G., and Phillips, O. L.: The RAIN-FOR database: monitoring forest biomass and dynamics, J. Veg. Sci., 18, 535–542, doi:10.1111/j.1654-1103.2007.tb02568.x, 2007.

Phillips, O. L., Baker, T. R., Arroyo, L., Higuchi, N., Killeen, T. J., Laurance, W. F., Lewis, S. L., Lloyd, J., Malhi, Y., Monteagudo, A., Neill, D. A., Núñez Vargas, P., Silva, J. N. M., Terborgh, J., Vásquez Martínez, R., Alexiades, M., Almeida, S., Brown, S., Chave, J., Comiskey, J. A., Czimczik, C. I., Di Fiore, A., Erwin, T., Kuebler, C., Laurance, S. G., Nascimento, H. E. M., Olivier, J., Palacios, W., Patiño, S., Pitman, N. C. A., Quesada, C. A., Saldias, M., Torres Lezama, A., and Vinceti, B.: Pattern and process in Amazon tree turnover, 1976–2001, Philos. T. Roy. Soc. B, 359, 381–407, doi:10.1098/rstb.2003.1438, 2004.

Phillips, O. L., Van Der Heijden, G., Lewis, S. L., López-González, G., Aragão, L. E. O. C., Lloyd, J., Malhi, Y., Monteagudo, A., Almeida, S., Dávila, E. A., Amaral, I., Andelman, S., Andrade, A., Arroyo, L., Aymard, G., Baker, T. R., Blanc, L., Bonal, D., De Oliveira, Á. C. A., Chao, K.-J., Cardozo, N. D., Da Costa, L., Feldpausch, T. R., Fisher, J. B., Fyllas, N. M., Freitas, M. A., Galbraith, D., Gloor, E., Higuchi, N., Honorio, E., Jiménez, E., Keeling, H., Killeen, T. J., Lovett, J. C., Meir, P., Mendoza, C., Morel, A., Vargas, P. N., Patiño, S., Peh, K. S. H., Cruz, A. P., Prieto, A., Quesada, C. A., Ramírez, F., Ramírez, H., Rudas, A., Salamão, R., Schwarz, M., Silva, J., Silveira, M., Ferry Slik, J. W., Sonké, B., Thomas, A. S., Stropp, J., Taplin, J. R. D., Vásquez, R., and Vilanova, E.: Drought–mortality relationships for tropical forests, New Phytol., 187, 631–646, doi:10.1111/j.1469-8137.2010.03359.x, 2010.

Quesada, C. A., Lloyd, J., Schwarz, M., Patiño, S., Baker, T. R., Czimczik, C., Fyllas, N. M., Martinelli, L., Nardoto, G. B., Schmerler, J., Santos, A. J. B., Hodnett, M. G., Herrera, R., Luizão, F. J., Arneth, A., Lloyd, G., Dezzeo, N., Hilke, I., Kuhlmann, I., Raessler, M., Brand, W. A., Geilmann, H., Moraes Filho, J. O., Carvalho, F. P., Araujo Filho, R. N., Chaves, J. E., Cruz Junior, O. F., Pimentel, T. P., and Paiva, R.: Variations in chemical and physical properties of Amazon forest soils in relation to their genesis, Biogeosciences, 7, 1515–1541, doi:10.5194/bg-7-1515-2010, 2010.

Quesada, C. A., Lloyd, J., Anderson, L. O., Fyllas, N. M., Schwarz, M., and Czimczik, C. I.: Soils of Amazonia with particular reference to the RAINFOR sites, Biogeosciences, 8, 1415–1440, doi:10.5194/bg-8-1415-2011, 2011.

Quesada, C. A., Phillips, O. L., Schwarz, M., Czimczik, C. I., Baker, T. R., Patiño, S., Fyllas, N. M., Hodnett, M. G., Herrera, R., Almeida, S., Alvarez Dávila, E., Arneth, A., Arroyo, L., Chao, K. J., Dezzeo, N., Erwin, T., di Fiore, A., Higuchi, N., Honorio Coro-

Title Page

Abstract | Introduction

Conclusions | References

Tables | Figures

|◄ | ►|

◄ | ►

Back | Close

Full Screen / Esc

Printer-friendly Version

Interactive Discussion

nado, E., Jimenez, E. M., Killeen, T., Lezama, A. T., Lloyd, G., López-González, G., Luizão, F. J., Malhi, Y., Monteagudo, A., Neill, D. A., Núñez Vargas, P., Paiva, R., Peacock, J., Peñuela, M. C., Peña Cruz, A., Pitman, N., Priante Filho, N., Prieto, A., Ramírez, H., Rudas, A., Salomão, R., Santos, A. J. B., Schmerler, J., Silva, N., Silveira, M., Vásquez, R., Vieira, I., Terborgh, J., and Lloyd, J.: Basin-wide variations in Amazon forest structure and function are mediated by both soils and climate, Biogeosciences, 9, 2203–2246, doi:10.5194/bg-9-2203-2012, 2012.

Saatchi, S. S., Harris, N. L., Brown, S., Lefsky, M., Mitchard, E. T. A., Salas, W., Zutta, B. R., Buermann, W., Lewis, S. L., Hagen, S., Petrova, S., White, L., Silman, M., and Morel, A.: Benchmark map of forest carbon stocks in tropical regions across three continents, Proc. Natl. Acad. Sci., 108, 9899–9904, doi:10.1073/pnas.1019576108, 2011.

Senna, M. C. A., Costa, M. H. C., Pinto, L. I. C., Imbuzeiro, H. M. A., Diniz, L. M. F., and Piriz, G. F.: Challenges to reproduce vegetation structure and dynamics in amazonia using a coupled climate-biosphere model, Earth Interact., 13, 1–28, doi:10.1175/2009EI281.1, 2009.

Sheffield, J., Goteti, G., and Wood, E. F.: Development of a 50-yr high-resolution global dataset of meteorological forcings for land surface modeling, J. Climate, 19, 3088–3111, doi:10.1175/JCLI3790.1, 2006.

Thompson, S. L. and Pollard, D.: A global climate model (GENESIS) with a Land-Surface Transfer Scheme (LSX), Part II: CO_2 sensitivity, J. Climate, 8, 1104–1121, doi:10.1175/1520-0442(1995)008<1104:agcmwa>2.0.CO;2, 1995a.

Thompson, S. L. and Pollard, D.: A global climate model (GENESIS) with a Land-Surface Transfer Scheme (LSX), Part I: present climate simulation, J. Climate, 8, 732–761, doi:10.1175/1520-0442(1995)008<0732:agcmwa>2.0.CO;2, 1995b.

Vitousek, P. M.: Litterfall, nutrient cycling, and nutrient limitation in tropical forests, Ecology, 65, 285–298, 1984.

Willmott, C. J.: Some comments on the evaluation of model performance, B. Am. Meteorol. Soc., 63, 1309–1313, 1982.

Amazon Heterogeneity

A. D. de Almeida Castanho et al.

**Amazon
Heterogeneity**

A. D. de Almeida
Castanho et al.

Table 1. List of field data used in this study with the respective reference in literature. The original number of plots from each study is presented in column A, the respective number of grid cells at 1° × 1° resolution is presented in column B. The methods for upscaling and the regression equations used are presented. The table is divided into field data used for input parameterization in the model and field data of woody net primary productivity and woody above-ground biomass used for model output validation (shaded cells).

Property (unit)	Paper	# plots (A)	# grid cells in studied region (B)	Method of Upscaling	Regression Equations
Model Parameterization					
Carbon allocation to wood, leaves and roots (fraction)	Malhi et al., 2011; Aragão et al., 2009	10	6	Based on Sand Fraction from Quesada et al., 2010 Soil Texture Map	Equation (1) $C_{root} = 0.0039 \cdot Sand(\%) + 0.137$; $R^2 = 0.97$; $p < 0.004$ $C_{leaf} = -0.0025 \cdot Sand(\%) + 0.44$; $R^2 = 0.69$; $p < 0.04$ $C_{wood} = 1 - C_{root} - C_{leaf}$
Woody Biomass Residence Time (yr)	Galbraith et al., 2012	129	34	Kriging Interpolation	-x-
Soil Total Phosphorus Content (P) (mg kg^{-1})	Quesada et al., 2010	71	26	Based on Quesada et al., 2011 Soil Class Map	(Soil total P site level) × (Soil Class Site Level) Fig. 4
Maximum carboxylation capacity of Rubisco (V_{cmax}) (µmol CO$_2$ m^{-2} s^{-1})	Fyllas et al., 2009 (Phosphorus leaf site)	62	22	Based on Soil total Phosphorus Map (above)	Equation (2) $V_{cmax} = 0.1013 \cdot P(mg\,kg^{-1}) + 30.037$; $R^2 = 0.77$; $p < 0.005$
Specific Leaf Area Index (SLA) (m^2 kg^{-1})	Fyllas et al., 2009	62	22	Kriging Interpolation	-x-
Model Output Validation data					
Woody Net Primary Productivity NPP$_w$ (kg C m^2 yr^{-1})	Malhi et al., 2004	104	25	-x-	-x-
Woody Above-ground Biomass AGB$_w$ (kg C m^{-2})	Malhi et al., 2006	227	69	-x-	-x-

11801

Table 2. Summary of the parameterization setup for each of the simulation experiments: the control simulation (CA) with the original IBIS prescribed homogeneous parameterization; the SA3a with corrected carbon allocation, with homogeneous parameterizations in space; site-level simulation (SS) with heterogeneous parameterizations represented; and the regional simulation (RS) with the upscale of the respective parameters.

		Homogeneous Parameterization		Heterogeneous Parameterizations	
		(CA) Control Simulation IBIS original setup	(SA3a) (CA) with Change in C allocation	(SS) Site-level Simulation Site observation data	(RS) Regional Simulation Regional estimated data
Carbon Allocation to wood, leaves and roots	%	Fixed space 50 % Wood, 30 % Leaves, 20 % Roots	Fixed space 34 % Wood, 33 % Leaves, 34 % Roots	Site function of Soil Texture Quesada et al. (2010)	Map Estimated Function Soil Texture map
Woody Biomass Residence Time	years	Fixed space 25	Fixed space 25	Site data from Galbraith et al. (2012)	Map Kriging interpolation Site data from Galbraith et al. (2012)
Maximum carboxylation capacity of Rubisco (V_{cmax})	$\mu mol\,CO_2\,m^{-2}\,s^{-1}$	Fixed space 75	Fixed space 75	Site estimate from Mercado et al., 2009	Map Estimated Function Soil Phosphorus Map
Specific Leaf Area Index (SLA)	$m^2\,kg^{-1}$	Fixed space 25	Fixed space 25	Site data from Fyllas et al. (2009)	Map Kriging interpolation Site data from Fyllas et al. (2009)

Table 3. Statistical summary of the comparison of woody net primary productivity between IBIS simulated results and field estimates. The table presents the number of data points within the studied area, mean and standard deviation, regression slope, intercept and correlation coefficient, and index of agreement (d). The statistical analyses were made for all sites excluding four outliers (JEN, CAQ, SCR, CUZ, discussed in Supplement D). The statistical analyses was divided in groups of data point as: Series A and B represent the series of all data points that have available NPP_w field information where Series A: represent the series of data where the V_{cmax} was estimated based on field information; Series B: represent all other data points where NPP_w field was known and V_{cmax} was extrapolated based on the methodology described in this work.

Woody NPP ($kg\,C\,m^{-2}\,yr^{-1}$)	# data poits	Mean (Stdev)	a slope (Stdev)	b intercept (Stdev)	Correlation Coefficient R	d index of agreement Willmott et al. (1982)
Observed Series A	10	0.31 (0.06)				
Observed Series B	9	0.27 (0.04)				
SA3a Series A	10	0.34 (0.03)	−0.04 (0.15)	0.35 (0.05)	−0.1	0
SA3a Series B	10	0.36 (0.03)	0.49 (0.14)	0.22 (0.04)	0.79	0.3
SS Series A	9	0.34 (0.05)	0.58 (0.20)	0.16 (0.07)	0.71	0.7
RS Series B	9	0.34 (0.04)	0.62 (0.30)	0.17 (0.08)	0.66	0.4

Table 4. Statistical summary of the comparison of wood above-ground biomass between IBIS simulated results and field estimates. The table presents the number of data points within the studied area, mean and standard deviation, regression slope, intercept and correlation coefficient, and index of agreement (d). The statistical analyses were made for all sites excluding three (CUZ, CHN and AMB, in Supplement D). The statistical analyses was divided in groups of data point as: Series C and D represent the series of all data points that have available AGB_w field information where Series C: represent the series of data where the woody residence time was estimated based on field information; Series D: represent all other data points where AGB_w field was known and woody residence time was extrapolated based on the methodology described in this work.

Woody AGB ($kg\,C\,m^{-2}$)	# data points	Mean (Stdev)	A slope (Stdev)	B intercept (Stdev)	Correlation Coefficient R	d index of agreement Willmott et al. (1982)
Observed Series C	21	15.4 (2.3)				
Observed Series D	42	14.3 (2.8)				
SA3a Series C	21	7.3 (0.5)	0.05 (0.05)	6.5 (0.8)	0.22	0
SA3a Series D	42	7.6 (0.6)	−0.002 (0.050)	7.6 (0.8)	−0.006	0
SS Series C	21	13.7 (2.3)	1.06 (0.18)	−2.8 (2.8)	0.80	0.8
RS Series D	42	13.1 (2.6)	0.44 (0.71)	6.9 (1.1)	0.52	0.6

Full Screen / Esc

Printer-friendly Version

Interactive Discussion
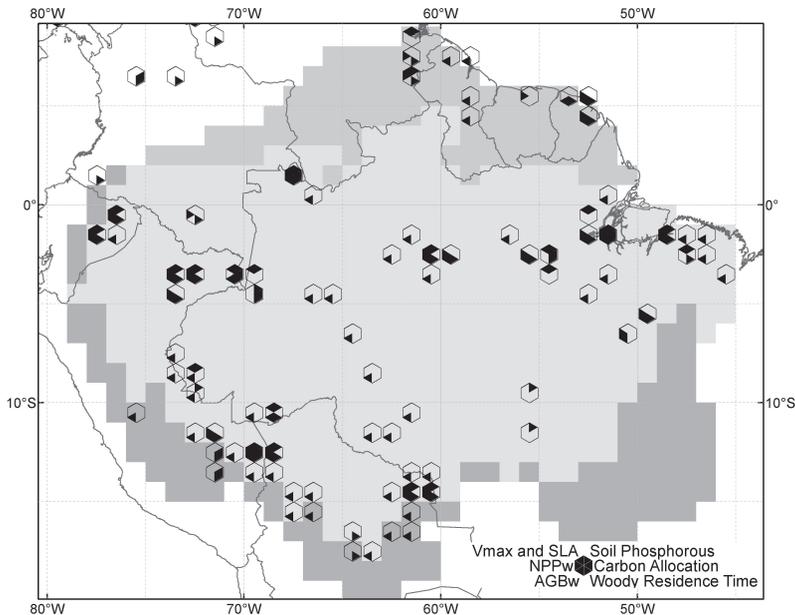
Fig. 1. Locations of the main field observation data: woody above-ground biomass (Malhi et al., 2006); woody net primary productivity (Malhi et al., 2004); maximum carboxylation capacity of Rubisco and specific leaf area index (Fyllas et al., 2009); soil total Phosphorus (Quesada et al., 2010); woody carbon allocation (Malhi et al., 2011); woody residence time (Galbraith et al., 2012). Shaded areas include the Amazonian *sensu sctricto* (Amazon basin below 700 m asl, light gray) with an estimated area ($\sim 5.65 \times 10^6$ km^2); Amazon River basin (light gray including southeast Planalto and Western Andes, dark gray) and tropical forest areas in the north (Guiana, dark gray) (Eva et al., 2005). Each field site that provided data is marked by a hexagon, which is divided into 6 wedges. Each wedge corresponds to a particular variable (see key in lower right). If a particular field variable is available at a site the wedge corresponding to it is black. For example if woody above-ground biomass (AGB$_w$) was collected at a particular site the lower left wedge is black.
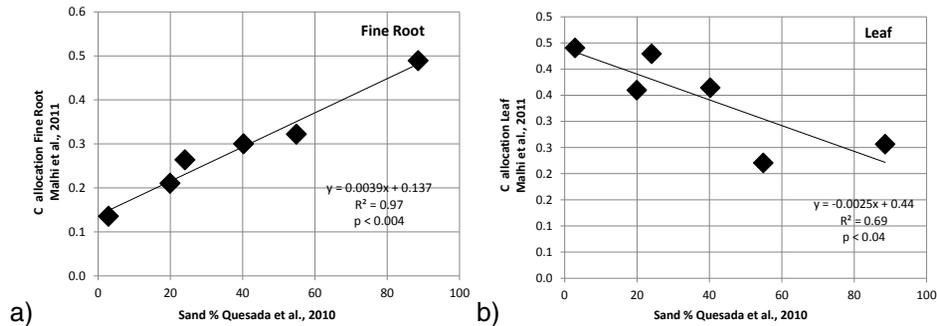
Fig. 2. The relationship between fraction of NPP allocation to fine roots and percentage of sand in soil **(a)**, same for carbon allocation to leaves and percentage of sand in soil **(b)** (Malhi et al., 2011; Quesada et al., 2010).
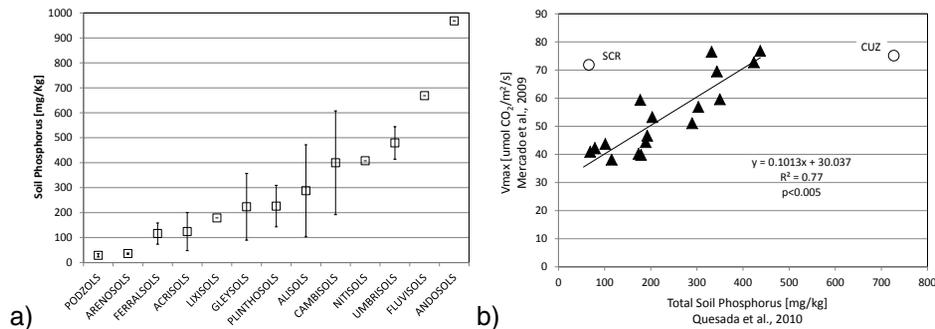
Fig. 3. (a) Total soil phosphorus agregated by soil type, based on field data from Amazonia, it is shown the average and standard deviation for each soil class; **(b)** regression between V_{cmax} (Mercado et al., 2009) and total soil P (average depth from 0 to 0.3 m); Quesada et al. (2010), excluding CUZ and SCR field site (Supplement D).
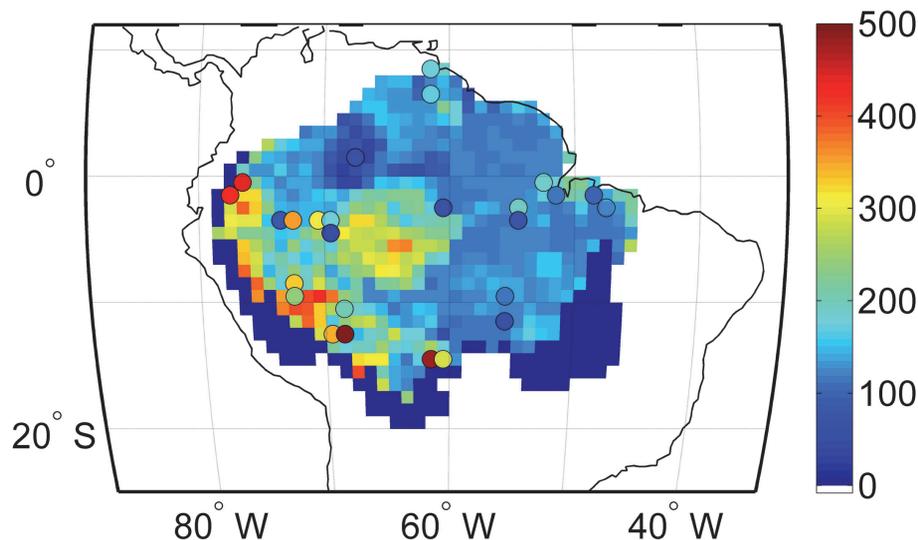
Fig. 4. Estimated total soil phosphorus map in mg/kg (average depth from 0 to 0.3 m). The dots represent averaged field plot measurements in one-degree grid cells (Quesada et al., 2010). The total soil phosphorus map (background) is derived based on soil class map and the relationship between site level total soil P content and soil class (Fig. 3).

Title Page

Abstract | Introduction

Conclusions | References

Tables | Figures

|◄ | ►|

◄ | ►

Back | Close

Full Screen / Esc

Printer-friendly Version

Interactive Discussion
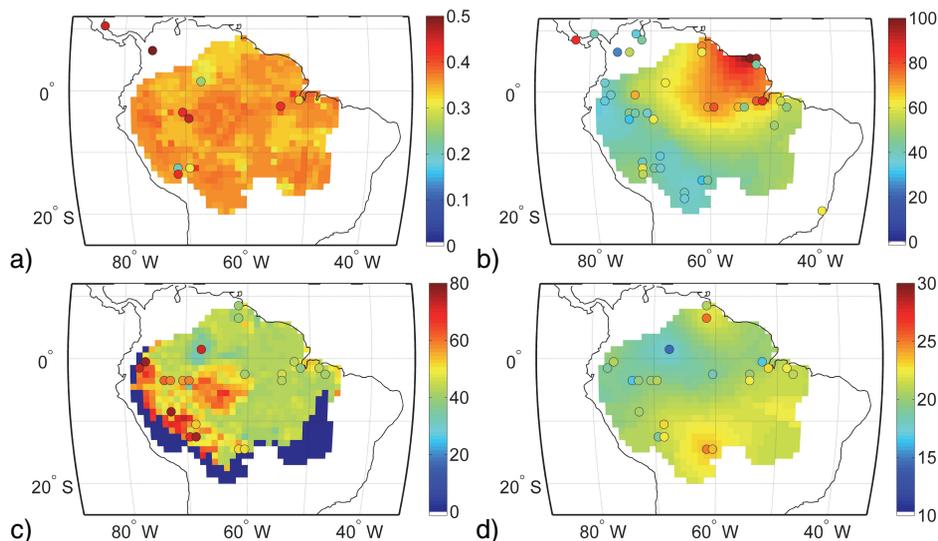
Fig. 5. Site specific field data (dots) and the extrapolated map (background): **(a)** carbon allocation to wood [fraction], where the extrapolated map is based on sand fraction map; **(b)** woody biomass residence time in years where the extrapolation is by kriging interpolation of site data; **(c)** maximum carboxylation capacity of Rubisco ($\mu mol\,CO_2\,m^{-2}\,s^{-1}$), where the extrapolation method is based on total soil P map; **(d)** specific leaf area index ($m^2\,kg^{-1}$), where the extrapolation is by kriging interpolation of site data.
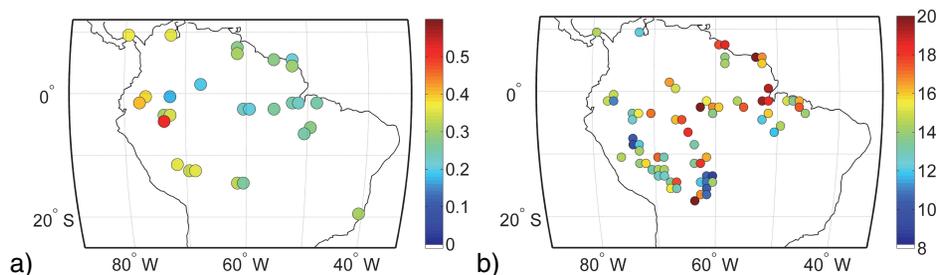
Fig. 6. (a) Estimated wood net primary productivity (NPP_w) ($kg\,C\,m^{-2}\,yr^{-1}$) and **(b)** wood live above-ground biomass (AGB_w) ($kg\,C\,m^{-2}$), based on field data by Malhi et al. (2004, 2006), respectively. Dots represent the average from measurement plots averaged to $1° \times 1°$ grid cell.
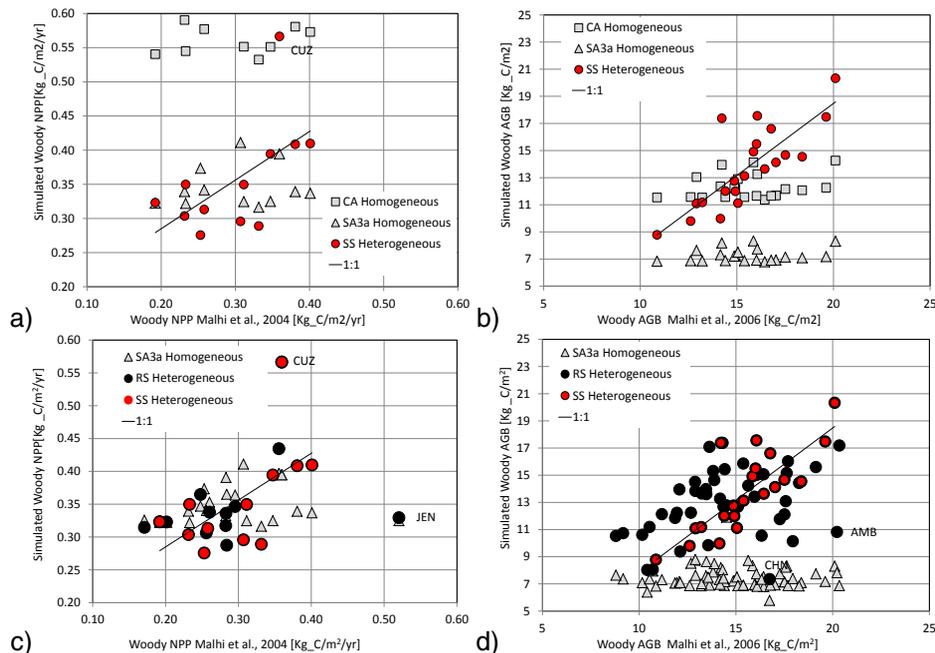
Fig. 7. Comparison of IBIS simulated values with field observations. Figures on the left **(a, c)** are comparisons of woody above-ground net primary productivity. Figures on the right **(b, d)** are comparisons of woody above-ground live biomass. Figures **(a)** and **(b)** are IBIS simulated results, only for grid cells where the V_{cmax} (Series A) and woody residence time (Series B) are known; while, **(c)** and **(d)** are the IBIS simulated results for the full series of data where NPP_w and AGB_w field data are available (Series A + B and C + D).
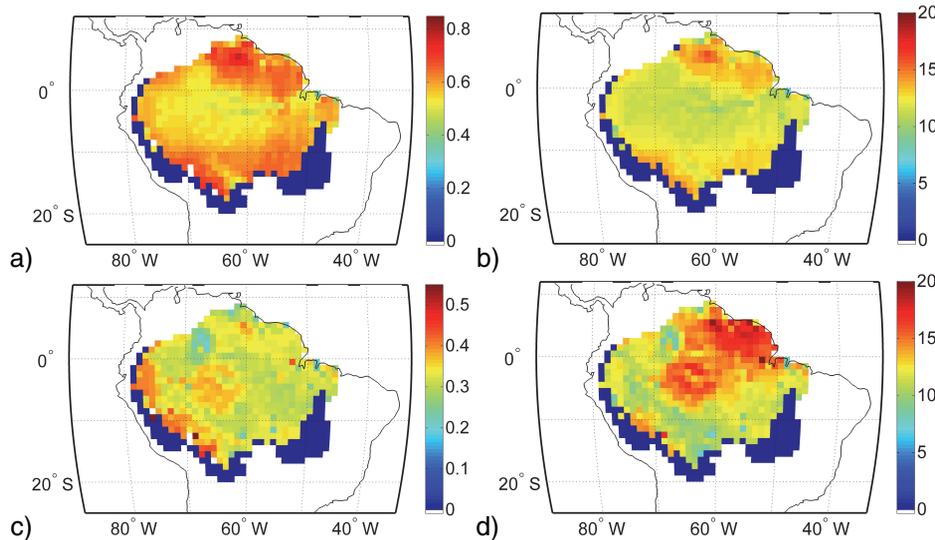
Fig. 8. Woody above-ground net primary productivity (left column) and the woody above-ground live biomass (right column). The first row presents the regional simulation under the control scenario (CA). The second row presents the IBIS simulated map based on the up scaled parameterization (RS).

**Amazon
Heterogeneity**

A. D. de Almeida
Castanho et al.

Fig. 9. Estimates of above-ground live biomass (including trees lower 10 cm dbh and lianas) in the Amazon tropical forest scaled to the 5.65×10^6 km^2 area of this study. The estimates are derived from satellite (Saatchi et al., 2011; Baccini et al., 2012; Houghton et al., 2001), field estimates (Malhi et al., 2006; Houghton et al., 2001) and numerical modeling simulation (IBIS, in this study). The numbers shown represent the above-ground biomass density estimated in each study (total C on above-ground biomass divided by the forest area) multiplied by our study area of 5.65×10^6 km^2.